Images of Illusory Motion in Primary Visual Cortex

Axel Larsen[1], Kristoffer H. Madsen[2,3], Torben E. Lund[2], and Claus Bundesen[1]

Abstract

■ Illusory motion can be generated by successively flashing a stationary visual stimulus in two spatial locations separated by several degrees of visual angle. In appropriate conditions, the apparent motion is indistinguishable from real motion: The observer experiences a luminous object traversing a continuous path from one stimulus location to the other through intervening positions where no physical stimuli exist. The phenomenon has been extensively investigated for nearly a century but little is known about its neurophysiological foundation. Here we present images of activations in the primary visual cortex in response to real and apparent motion. The images show that during apparent motion, a path connecting the cortical representations of the stimulus locations is filled in by activation. The activation along the path of apparent motion is similar to the activation found when a stimulus is presented in real motion between the two locations. ■

INTRODUCTION

In a classical paradigm for investigating visual apparent motion, two spatially separated stationary spots of light are presented in sequential alternation. When the rate of alternation is not too fast, and the spatial separation is not too large, the human observer perceives a single spot of light moving smoothly (''continuously'') back and forth over the straight path between the two positions of presentation (Larsen, Farrell, & Bundesen, 1983; Kolers, 1972; Korte, 1915; Wertheimer, 1912). The strength of the illusion depends on the distance between the two positions. At very small spatial separations, apparent motion is indistinguishable from real motion (De Silva, 1929). At larger separations, the illusion is weaker, but vivid apparent motion can be experienced over spatial separations subtending several degrees of visual angle (Larsen, Farrell, et al., 1983; De Silva, 1929).

There is psychological and neurobiological evidence of at least two distinct systems for analysis of visual motion in man (Zhuo et al., 2003; Larsen, Farrell, et al., 1983; Anstis, 1980; Braddick, 1980): a short-range system that analyzes small spatial displacements (0.25° or below) across the retina, and a long-range system that captures large displacements. The short-range system may be based on banks of low-level motion energy filters (Adelson & Bergen, 1985), which are bypassed by the long-range system. In the study of apparent motion reported here, the spatial separation between the stimuli (2.9°) was larger than the receptive fields in the primary visual cortex (Pack, Born, & Livingstone, 2003) and more than an order of magnitude beyond the operating range of the short-range system. However, the separation was sufficiently small to give long-range apparent motion that looked like real motion.

Our experiments were done in a 3-T functional magnetic resonance imaging (fMRI) environment in which visual stimuli were rear-projected to the observer by means of a mirror mounted on the head coil. During the scans, observers maintained fixation at a small point in the middle of the display. In the baseline condition, only the fixation point was displayed. All stimulus displays shown in the four experimental conditions were symmetrical about the fixation point (see Figure 1). In the apparent motion condition, either side of the stimulus display showed two dots flashing in sequential alternation at a rate of 1.25 Hz, which produced optimal apparent motion, back and forth, over a path subtending 2.9° of visual angle. In the flashing dots condition, the displays were exactly the same except that the two dots flashed in synchrony rather than sequential alternation. Thus, each dot was flashed at just the same rate in the flashing dots condition as in the apparent motion condition. In the flashing bar condition, a bar was flashed at a rate of 1.25 Hz on either side of the display. The bar coincided with the path of apparent motion between the stimulus locations used in the apparent motion and flashing dots conditions. In the real motion condition, a dot was presented in nearly continuous motion, back and forth, in either side of the display. The trajectory coincided with the path of apparent motion in the apparent motion condition

[1]University of Copenhagen, Denmark, [2]Copenhagen University Hospital, Denmark, [3]Technical University of Denmark, Denmark

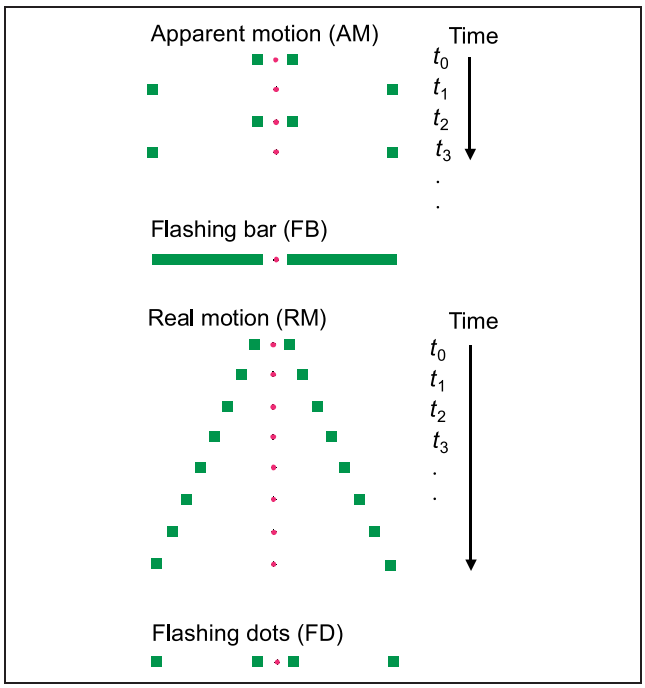

Figure 1. Experimental conditions: apparent motion, flashing bar, real motion, and flashing dots. The stimulus displays (green squares and rectangular bars) were symmetrical about the fixation point (red circle). The figure is not drawn to scale.

and the bar shown in the flashing bar condition. Stimulus presentations were blocked by condition, and the total luminous energy emitted from the stimulus display was kept constant across the experimental conditions. During separate scans, the primary visual cortex (area V1) was located in both hemispheres by standard techniques using a rotating wedge (polar) and an expanding/contracting ring (eccentricity) stimulus (Sereno et al., 1995).

METHODS

Participants

Six right-handed members of staff or graduate students of psychology, two men and four women, were recruited to participate in the study. The mean age was 26.5 years (range, 20–31 years). Informed written consent was obtained using a consent form approved by the Ethical Committee of Copenhagen and Frederiksberg (KF 01-131/03).

Stimuli and Design

Stimuli were rear-projected to the observer in the scanner from an LCD projector by means of a mirror mounted on the head coil. In this setup, 42 pixels on the LCD projector subtended a visual angle of 1°. In the center of the display, a small, red fixation point (one pixel) was permanently displayed. There were five stimulus conditions: fixation-point alone (baseline), apparent motion, flashing bar, real motion, and flashing dots. Each observer participated in one scan, which comprised 10 consecutive 75-sec periods such that each period contained one 15-sec presentation of each of the five stimulus conditions. The temporal parameters in the four experimental conditions were chosen so that the total luminous energy emitted from the stimulus display was kept constant across the experimental conditions.

All stimulus displays were symmetrical about both the vertical and the horizontal meridian (cf. Figure 1). In the apparent motion condition, either side (left vs. right) of the stimulus display showed two small (7 × 7 pixels) green squares in sequential alternation. One of the squares was centered at a distance of 8 pixels from the vertical meridian, the other square was centered at a distance of 132 pixels from the vertical meridian. The horizontal displacement between the two squares (124 pixels) subtended a visual angle of 2.9°. Each square was exposed for 400 msec, and the exposures of the two squares alternated without any intervening blank interval. Thus, the stimulus-onset asynchrony was 400 msec, the interstimulus interval was 0 msec, and the full stimulus cycle took 800 msec corresponding to a repetition rate of 1.25 Hz. The flashing dots condition was identical to the apparent motion condition except that the exposures of the squares were synchronized such that the full stimulus cycle consisted of a 400-msec exposure of four green squares followed by a blank interval of 400 msec.

In the flashing bar condition, either side of the display showed a flashing green horizontal bar. The bar was rectangular with a length of 131 pixels and a width of 7 pixels. The left end (7 × 7-pixel area) of the bar in the left visual field was positioned at the location of the leftmost green (7 × 7 pixels) square used in the apparent motion condition, whereas the right end of the bar was positioned at the location of the rightmost green square used in the left visual field in the apparent motion condition. A full 800-msec stimulus cycle consisted of a 58-msec exposure of the two bars followed by a blank interval of 742 msec.

In the real motion condition, either side of the display showed a green (7 × 7 pixels) square moving back and forth between the two stimulus locations used in the apparent motion condition. At the beginning of a full 800-msec stimulus cycle, the square was displayed centered at a distance of 8 pixels from the vertical meridian. By the next refresh cycle, the square was shifted 4 pixels away from the vertical meridian. The shift was repeated until the square had moved a distance of 124 pixels (4 pixels by each new refresh). At this point, the direction of motion was reversed, and the square moved back to the initial position at a rate of 4 pixels per refresh.

fMRI Acquisition

MRI was performed on a 3-T MR scanner (Magnetom Trio, Siemens, Erlangen, Germany) equipped with the standard birdcage head coil. The functional images were acquired using an echo planar imaging (EPI) GE sequence including PACE (Thesen, Heid, Mueller, & Schad, 2000). The functional volumes consisted of 26 3-mm slices oriented along the calcarine sulcus with the following acquisition parameters: TR = 1.55 sec, TE = 30 msec, FOV = 192 × 192 mm, 64 × 64 matrix, flip angle = 72°.

The observers' heads were supported by means of a vacuum cushion and foam pads. Structural scans were acquired using an MPRAGE and consisted of 192 sagittal 1-mm slices with 256 × 256 acquisition matrix, FOV = 256 × 256 mm, TR = 1.55 sec, TE = 3.93 msec.

fMRI Analysis

All preprocessing and analysis steps were conducted using BrainVoyager QX (Brain Innovation, Maastricht, the Netherlands). Preprocessing included 3-D motion correction by a six-parameter rigid body transformation of the time series followed by high-pass filtering with 1/150 Hz cutoff frequency. The EPI volumes were coregistered to the structural scan using a rigid body transformation. To ease segmentation and cortical surface extraction, the structural scans were normalized into Talairach space (Talairach & Tournoux, 1988) using a nine-parameter affine transformation.

Data analysis was performed by means of the general linear model (GLM). The four predictors corresponding to the four experimental conditions—flashing dots (FD), flashing bar (FB), real motion (RM), and apparent motion (AM)—were constructed by convolving a function indicating the activation type (one during activation, zero otherwise) with the expected hemodynamic impulse response function: a gamma function with shape parameter $n = 3$ and scale parameter (time constant) $\tau = 1.25$ sec, shifted by a pure delay of $\delta = 2.5$ sec (cf. Boynton, Engel, Glover, & Heeger, 1996). Prior to computation of maximum likelihood estimates of the regression coefficients (β_{FD}, β_{FB}, β_{RM}, and β_{AM}), temporal autocorrelation was accounted for by using the first-order autoregressive model correction method implemented in BrainVoyager.

To test for the effect of apparent motion in the primary visual cortex, we first delineated V1 using retinotopic maps and the location of the calcarine sulcus. In V1 we next defined a region of interest (ROI) by the activity trace ($z > 1.5$) generated by real motion (RM condition relative to the fixation-point baseline condition). For the ROI in each hemisphere of each observer, the GLM model was then refitted to obtain estimates of the contrast $\beta_{AM} - \beta_{FD}$. These parameter estimates were subsequently used in a second-level analysis to test the hypothesis that the activity due to apparent motion exceeded the activity due to flashing dots (i.e., $\beta_{AM} - \beta_{FD} > 0$). The hypothesis was tested by one-tailed pairwise t tests across the six observers (see Table 1). Measures of $\beta_{AM} - \beta_{FD}$ outside the activity spots due to the flashing dots were obtained by further restricting the ROI to voxels with $z < 1.5$ in the flashing dots condition and refitting the GLM model to the restricted ROI.

We estimated mean locations of activations in the MT complex during both real and apparent motion. The locations were estimated as the centers of gravity of activated ($p < .05$, false-discovery-rate corrected; Genovese, Lazar, & Nichols, 2002) voxel clusters that were greater than 50 mm^3 and located near the junction of the temporal, occipital, and parietal lobes (see Table 2). The clusters corresponding to activations in the MT complex during real motion were used as ROIs in a further analysis in which the GLM model was refitted to these ROIs to obtain estimates of β_{FD}, β_{FB}, β_{RM}, and β_{AM} in the MT complex (see Table 3).

Table 1. ROI Analysis of Regression Coefficients in V1

	Left Hemisphere			*Right Hemisphere*		
Observer	β_{AM}	β_{FD}	$\beta_{AM} - \beta_{FD}$	β_{AM}	β_{FD}	$\beta_{AM} - \beta_{FD}$
1	0.334	−0.066	0.400	−0.087	−0.473	0.385
2	0.570	0.152	0.418	0.712	0.287	0.425
3	0.143	0.098	0.046	0.535	−0.035	0.570
4	0.060	−0.107	0.167	0.233	0.098	0.135
5	0.605	0.255	0.350	0.338	−0.079	0.417
6	0.012	−0.544	0.555	0.545	−0.292	0.838
Mean	0.287	−0.035	0.323*	0.379	−0.082	0.462*

*$p < .005$ by one-tailed pairwise t test of the hypothesis that $\beta_{AM} - \beta_{FD} = 0$.

Table 2. Centers of Activation in MT+ during Real and Apparent Motion

	Left Hemisphere[a]			*Right Hemisphere*[a]		
Observer	*x*	*y*	*z*	*x*	*y*	*z*
Real motion						
1	−49	−63	−6	46	−57	−7
2	−48	−68	1	44	−64	−4
3	−45	−59	1	51	−60	0
4	−46	−51	4	44	−59	−2
5	−47	−66	−2	42	−70	−4
6	−46	−76	3	47	−71	−7
Mean	−47	−64	0	46	−64	−4
SD	2	9	3	3	6	3
Apparent motion						
1	−50	−64	−5	47	−58	−7
2	−42	−76	−1	41	−70	−3
3	−48	−60	0	50	−62	0
4	−46	−51	3	42	−58	−3
5	−45	−66	−2	35	−75	−6
6	−46	−76	3	36	−77	−8
Mean	−46	−67	0	43	−67	−5
SD	3	10	3	6	8	3

[a]Talairach coordinates.

Retinotopic Mapping

Retinotopic mapping was obtained using a rotating wedge (polar) and an expanding/contracting ring (eccentricity) stimulus (Sereno et al., 1995). The stimuli were presented as parts of a flickering checkerboard on a gray background with a small fixation point (0.02°) at the center of the screen. The checkers reversed black/white at 8 Hz and were scaled by the cortical magnification factor ($A = 20, E = 0.5$) with expected coverage of 3-mm cortex per checker radially (Popovic & Sjöstrand, 2001). The polar mapping consisted of a 12° wedge rotating counterclockwise, performing one full rotation in 30 sec. This stimulus was shown for 4 min followed by a 30-sec rest period (fixation point only). Subsequently the same stimulus was presented in clockwise rotation (eight rotations, 4 min). Similarly, the eccentricity mapping consisted of an expanding/contracting ring covering one check radially with a cycle time of 30 sec (4 min expanding, 30 sec rest, 4 min contracting). Preprocessing parameters were similar to those of the apparent motion paradigm except that we used a high-pass filter with a cutoff frequency of 1/128 Hz.

The analysis was performed using a GLM with the first two harmonics of the stimulus cycle frequency as predictors. Activation phases (positions in the visual field) were found by means of the time to peak of the reconstructed signal. Averaging the two activation phases from stimuli moving in opposite directions eliminated the effects of the hemodynamic lag (including spatial variation) and differences in slice acquisition time.

RESULTS

Results from the left hemispheres of two observers are displayed in Figures 2 and 3. In Figures 2A and 3A, the blood oxygenation level dependent (BOLD) response in the primary visual cortex due to the flashing dots is clearly visible, close to the estimated representation of the horizontal meridian in the calcarine sulcus. The BOLD response to flashing dots is repeated in B–D of either figure. In addition to the BOLD response to flashing dots, B shows the contrast (difference image)

Table 3. ROI Analysis of Regression Coefficients in MT+

	Left Hemisphere				*Right Hemisphere*			
Observer	β_{AM}	β_{RM}	β_{FB}	β_{FD}	β_{AM}	β_{RM}	β_{FB}	β_{FD}
1	1.474	2.059	1.174	0.695	1.518	1.757	0.910	0.615
2	2.063	1.600	0.961	1.081	1.822	1.384	0.681	0.958
3	1.445	1.671	0.999	0.487	1.417	1.537	1.001	0.633
4	1.403	1.725	0.895	0.454	1.632	2.079	1.177	1.097
5	0.999	1.566	0.576	0.094	1.026	1.444	0.539	0.418
6	1.706	1.610	1.394	0.477	1.581	1.527	1.428	0.550
Mean	1.515	1.705	1.000	0.548	1.499	1.621	0.956	0.712

By two-tailed pairwise *t* tests, the hypotheses that $\beta_{AM} = \beta_{FB}$, $\beta_{AM} = \beta_{FD}$, $\beta_{RM} = \beta_{FB}$, and $\beta_{RM} = \beta_{FD}$ were all rejected for both left and right hemisphere comparisons ($p < .01$). Activations due to real and apparent motion were not reliably different in either hemisphere ($p > .30$). Flashing bar activation was significantly different from flashing dot activation in the left hemisphere ($p < .05$).

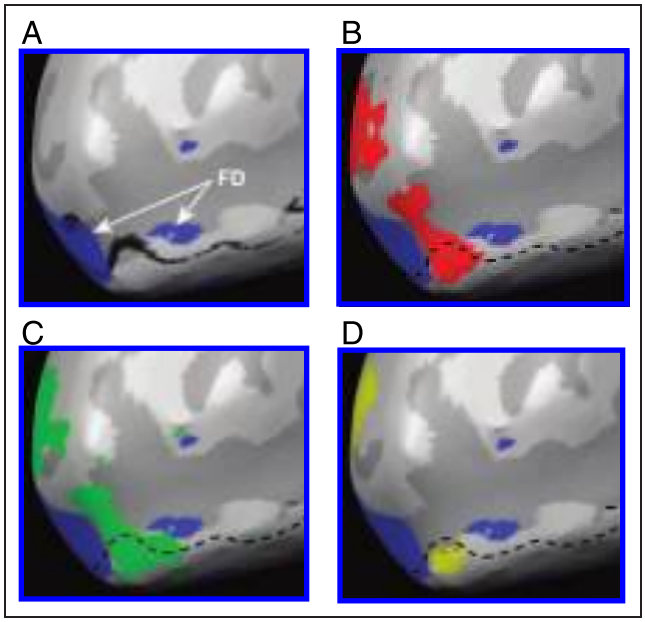

Figure 2. Cortical activations in 31-year-old male observer. The activations appear as colored patches on the inflated left occipital hemisphere. Gyri are indicated by light gray and sulci by darker gray. (A) BOLD response (blue) due to flashing dots (FD) relative to a baseline formed by the BOLD response in the fixation-point condition. The computed location of the representation of the horizontal meridian in the calcarine sulcus is shown in black. The computation was based on the mean activation caused by the rotating wedge passing through the horizontal orientation (mean of clockwise and counterclockwise rotations). (B) Contrast (red) between BOLD response to flashing bar and BOLD response to flashing dots along with the (blue) BOLD response to the flashing dots. The approximate location of the representation of the horizontal meridian in the calcarine sulcus is indicated by the dashed black line. (C) Contrast (green) between BOLD response to real motion and BOLD response to flashing dots along with the (blue) BOLD response to the flashing dots. (D) Contrast (yellow) between BOLD response to apparent motion and BOLD response to flashing dots along with the (blue) BOLD response to the flashing dots. For all activations, $p < .05$, uncorrected.

between the BOLD response to the flashing bar and the response to flashing dots, C shows the contrast between the BOLD response to real motion and the response to flashing dots, and D shows the contrast between the BOLD response to apparent motion and the response to flashing dots. The patches of activity between the neural representations of the flashing dots are strikingly similar, whether they are caused by the flashing bar, a moving spot of light, or a spot of light that just appears to move. A similar pattern of activity was observable in all of the six observers we tested.[1]

The BOLD response in a region of interest in V1 defined by the voxels activated by the real motion condition was reliably stronger in the apparent motion condition than in the flashing dots condition (see Table 1). For the ROI as a whole, the estimate of $\beta_{AM} - \beta_{FD}$, averaged across hemispheres, ranged between 0.151 and 0.697 across the six participants. With a mean of 0.392 and a standard error of the mean equal to 0.073, $\beta_{AM} - \beta_{FD}$ was highly significantly greater than zero; $t(5) = 5.39$, $p < .002$. For that part of the ROI that was outside the activity spots due to the flashing dots, the mean of $\beta_{AM} - \beta_{FD}$ was even greater (0.427) and the standard error of the mean was even smaller (0.070).

In agreement with previous findings (e.g., Larsen, Kyllingsbæk, Law, & Bundesen, 2005; Muckli et al., 2002; Tootell et al., 1995; Watson et al., 1993), our data also showed that both real and apparent motion caused reliable BOLD responses in the human motion processing complex (the MT complex, MT+). The estimated mean locations of voxels in activated clusters covering MT+ during real motion were (46, −64, −4) and (−47, −64, 0) in Talairach space. The corresponding mean locations during apparent motion were (43, −67, −5) and (−46, −67, 0), respectively (see Table 2). Thus, the estimated centers of MT+ activation due to real and apparent motion were close to each other. The strength of the MT+ activations due to real and apparent motion were not significantly different, but both activations were significantly stronger than the activations due to the flashing bar and the flashing dots (see Table 3).

DISCUSSION

Our findings fit in with the following three-stage theory of perception of long-range apparent motion (Bundesen, Larsen, & Farrell, 1983; Ullman, 1979; Beck, Elsner, & Silverstein, 1977). First, given two successive images of a

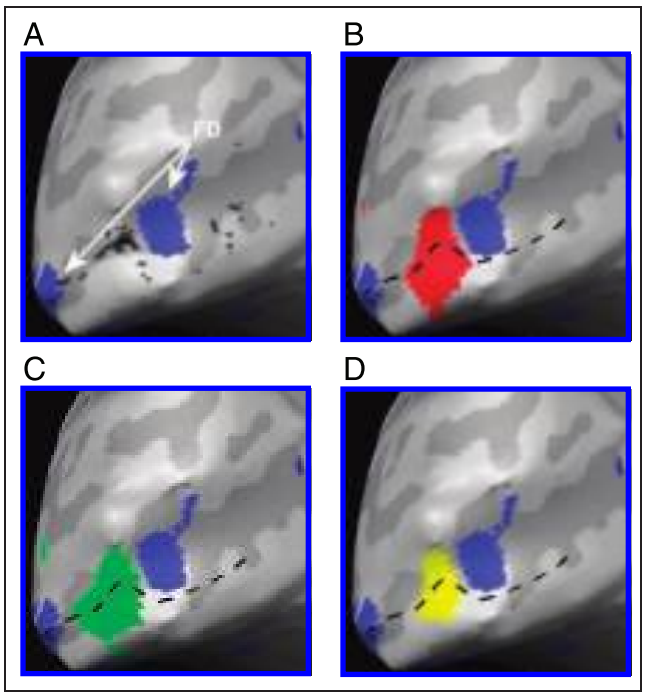

Figure 3. Cortical activations in 23-year-old female observer. The activations appear as colored patches on the inflated left occipital hemisphere. Conventions are the same as in Figure 2.

scene, the visual system identifies corresponding parts of the two images as successive views of the same objects. Second, when the ''correspondence problem'' has been solved, the system computes the motion intervening between the two presentations. Finally, for each pair of views of the same object, the computed motion trajectory is filled in by generation of a sequence of visual representations of the object in successive positions along the path from the position indicated by the first image to the position indicated by the second one—a sequence of representations similar to those that would have been generated if the object had been viewed in real motion over the trajectory.[2] Both the solution of the correspondence problem and the specification of the motion intervening between the stimulus presentations are generated by higher level visual areas, most likely the MT complex (Larsen, Kyllingsbæk, et al., 2005; Pascual-Leone & Walsh, 2001), but the perceptual filling-in is implemented in lower level visual areas by feedback connections from the higher level areas. Our data show that in appropriate conditions, the filling-in occurs at a level of processing as low as (or lower than) V1.

It is interesting to speculate on the functions of the perceptual filling-in (cf. Bundesen et al., 1983). Assuming that the process consists in generating a sequence of more or less sketchy representations of the stimulus object in successive positions along the computed motion trajectory, the process may stimulate short-range motion detectors in V1. If so, the process may be regarded as a normalization of the internal representation of an object viewed in apparent motion (i.e., with discrete presentations) to the format used for objects viewed in real motion. Following normalization of long-range discrete input to real-motion format, the perceptual routines used in analyzing representations of objects viewed in real motion may be directly applied to representations of objects seen in apparent motion. This way, the filling-in process in long-range apparent motion may serve economy of processing in the visual system as a whole.

Several types of evidence support the conjecture that long-range apparent motion is generated by interaction between MT+ and V1. More than three decades of research on the primate visual system has established that MT+ is critically involved in processing of visual motion, and MT+ and V1 communicate directly and reciprocally over a broad band of fibers (Rockland, 2004; Cornette et al., 1998; Shipp & Zeki, 1989). A particularly suggestive finding is that transcranial magnetic stimulation (TMS) of MT+ can induce visual sensations of moving phosphenes (spots of light), but the sensations of motion fail to appear if a TMS pulse is delivered over V1 some 30 msec later (Pascual-Leone & Walsh, 2001). This latency roughly corresponds to the time needed for communicating a signal from MT+ back to V1. There is also evidence that MT+ is implicated in perception of retinal stimuli as successive views of the same object at different locations, whether or not the views get connected by apparent motion (Larsen, Kyllingsbæk, et al., 2005), and evidence suggesting that MT+ is activated when motion is merely implied and may be inferred from static stimuli (Kourtzi & Kanwisher, 2000). MT+ activation by itself seems insufficient for generating sensations of motion.

Three recent studies that were conducted in parallel with the present study bear directly on our finding of perceptual filling-in in the primary visual cortex during apparent motion. Jancke, Chavane, Naaman, and Grinvald (2004) presented anesthetized cats with a briefly exposed square (''cue'') followed by a stationary line that extended away from the square. Although the line was presented all at once, human observers shown the same stimuli perceived illusory motion as though the line was being drawn from the cued end toward the uncued end (''line-motion illusion''). Jancke et al. recorded the time course of sub- and suprathreshold synaptic potentials in early visual cortex by voltage sensitive dye (VSD) imaging in the cats. The spatiotemporal course of the synaptic potentials in the cat's visual cortex was nearly the same during the line-motion illusion as during direct perception of a square in real motion along the path marked by the line. With the VSD technique, it could not be determined whether the effect was present in primary visual cortex in the anesthetized cats, but the results fit in with our demonstration of perceptual filling-in in the primary visual cortex during illusory motion in humans.

Liu, Slotnick, and Yantis (2004) investigated long-range apparent motion generated by two concentric circles presented in sequential alternation. The spatial separation of the circumferences of the two circles was nearly 5° of visual angle. With this large separation, BOLD signals in the MT complex were higher in amplitude during apparent motion than during flicker, but BOLD signals in the path of apparent motion in early visual areas were nearly the same during apparent motion and flicker. Thus, in primary visual cortex, filling-in was not noticeable.

By contrast, in a very recent article, using a paradigm highly similar to our own, Muckli, Kohler, Kriegeskorte, and Singer (2005) reported evidence of perceptual filling-in in the primary visual cortex during apparent motion over a visual angle as large as 18°. Furthermore, in a variation of the paradigm that used a bistable motion display, Muckli et al. confirmed that the activity was related to the conscious perception of motion.

Taken together, the results are consistent with the following conjectures. Long-range apparent motion that looks like real motion implicates activity in the primary visual cortex along a path connecting the representations of the stimulus locations. The strength of the illusion increases with the extent of this filling-in. Apparent motion over large visual angles is generally weaker than

motion over small angles, but there are cases in which vivid apparent motion is experienced over large spatial separations, and such cases are distinguished by noticeable filling-in in the primary visual cortex.

Acknowledgments

This research was supported by grants from the Danish Research Council for the Humanities and the Danish Research Agency. We thank Olaf B. Paulson for generous support during all phases of the project.

Reprint requests should be sent to Axel Larsen, Center for Visual Cognition, Department of Psychology, University of Copenhagen, DK-1361 Copenhagen K, Denmark, or via e-mail: larsen@psy.ku.dk.

The data reported in this experiment have been deposited with the fMRI Data Center (www.fmridc.org). The accession number is 2-2006-121QC.

Notes

1. A similar analysis of filling-in in visual area V2 seemed not feasible. We could not clearly separate the activations generated by each of the flashing dots in areas other than V1.
2. The successive positions need not be represented at neighboring locations in the cortex. Thus, in apparent motion across the vertical meridian, the representation in V1 of the moving object jumps from one hemisphere to the other one.

REFERENCES

Adelson, E. H., & Bergen, J. R. (1985). Spatiotemporal energy models for the perception of motion. *Journal of the Optical Society of America A, Optics, Image Science, and Vision, 2,* 284–299.

Anstis, S. M. (1980). The perception of apparent movement. *Philosophical Transactions of the Royal Society of London, Series B, 290,* 153–168.

Beck, J., Elsner, A., & Silverstein, C. (1977). Position uncertainty and the perception of apparent movement. *Perception & Psychophysics, 21,* 33–38.

Boynton, G. M., Engel, S. A., Glover, G. H., & Heeger, D. J. (1996). Linear systems analysis of fMRI in human V1. *Journal of Neuroscience, 16,* 4207–4221.

Braddick, O. (1980). Low-level and high-level processes in apparent motion. *Philosophical Transactions of the Royal Society of London, Series B, 290,* 137–151.

Bundesen, C., Larsen, A., & Farrell, J. E. (1983). Visual apparent movement: Transformations of size and orientation. *Perception, 12,* 549–558.

Cornette, L., Dupont, P., Spileers, W., Sunaert, S., Michiels, J., Van Hecke, P., Mortelmans, L., & Orban, G. A. (1998). Human cerebral activity evoked by motion reversal and motion onset. *Brain, 121,* 143–157.

De Silva, H. R. (1929). An analysis of the visual perception of movement. *British Journal of Psychology, 19,* 268–305.

Genovese, C. R., Lazar, N. A., & Nichols, T. (2002). Thresholding of statistical maps in functional neuroimaging using the false discovery rate. *Neuroimage, 15,* 870–878.

Jancke, D., Chavane, F., Naaman, S., & Grinvald, A. (2004). Imaging cortical correlates of illusion in early visual cortex. *Nature, 428,* 423–426.

Kolers, P. A. (1972). *Aspects of motion perception.* Oxford: Pergamon Press.

Korte, A. (1915). Kinematoskopische Untersuchungen. *Zeitschrift für Psychologie, 72,* 193–296.

Kourtzi, Z., & Kanwisher, N. (2000). Activation in human MT/MST by static images with implied motion. *Journal of Cognitive Neuroscience, 12,* 48–55.

Larsen, A., Farrell, J. E., & Bundesen, C. (1983). Short- and long range processes in visual apparent movement. *Psychological Research, 45,* 11–18.

Larsen, A., Kyllingsbæk, S., Law, I., & Bundesen, C. (2005). Activation in the MT-complex during visual perception of apparent motion and temporal succession. *Neuropsychologia, 43,* 1060–1071.

Liu, T., Slotnick, S. D., & Yantis, S. (2004). Human MT+ mediates perceptual filling-in during apparent motion. *Neuroimage, 21,* 1772–1780.

Muckli, L., Kriegeskorte, N., Lanfermann, H., Zanella, F. E., Singer, W., & Goebel, R. (2002). Apparent motion: Event-related functional magnetic resonance imaging of perceptual switches and states. *Journal of Neuroscience, 22,* RC219.

Muckli, L., Kohler, A., Kriegeskorte, N., & Singer, W. (2005). Primary visual cortex activity along the apparent-motion trace reflects illusory perception. *PLoS Biology, 3,* 1501–1510.

Pack, C. C., Born, R. T., & Livingstone, M. S. (2003). Two-dimensional substructure of stereo and motion interactions in macaque visual cortex. *Neuron, 37,* 525–535.

Pascual-Leone, A., & Walsh, V. (2001). Fast backprojections from the motion to the primary visual area necessary for visual awareness. *Science, 292,* 510–512.

Popovic, Z., & Sjöstrand, J. (2001). Relationship of receptive field estimates and resolution in the human retina. *Vision Research, 41,* 1313–1319.

Rockland, K. S. (2004). Feedback connections: Splitting the arrow. In J. H. Kaas & C. E. Collins (Eds.), *The primate visual system* (pp. 387–405). Boca Raton, FL: CRC Press.

Sereno, M. I., Dale, A. M., Reppas, J. B., Kwong, K. K., Belliveau, J. W., Brady, T. J., Rosen, B. R., & Tootell, R. B. (1995). Borders of multiple visual areas in humans revealed by functional magnetic resonance imaging. *Science, 268,* 889–893.

Shipp, S., & Zeki, S. (1989). The organization of connections between areas V5 and V1 in macaque monkey visual cortex. *European Journal of Neuroscience, 1,* 309–332.

Talairach, J., & Tournoux, P. (1988). *Co-planar stereotaxic atlas of the human brain.* New York: Thieme.

Thesen, S., Heid, O., Mueller, E., & Schad, L. R. (2000). Prospective acquisition correction for head motion with image-based tracking for real-time fMRI. *Magnetic Resonance in Medicine, 44,* 457–465.

Tootell, R. B. H., Reppas, J. B., Kwong, K. K., Malach, R., Born, R. T., Brady, T. J., Rosen, B. R., & Belliveau, J. W. (1995). Functional analysis of human MT and related visual cortical areas using magnetic resonance imaging. *Journal of Neuroscience, 15,* 3215–3230.

Ullman, S. (1979). *The interpretation of visual motion.* Cambridge: MIT Press.

Watson, J. D. G., Myers, R., Frackowiak, R. S. J., Hajnal, J. V., Woods, R. P. Mazziotta, J. C., Shipp, S., & Zeki, S. (1993). Area V5 of the human brain: Evidence from a combined study using positron emission tomography and magnetic resonance imaging. *Cerebral Cortex, 3,* 79–94.

Wertheimer, M. (1912). Experimentelle Studien über das Sehen von Bewegung. *Zeitschrift für Psychologie, 61,* 161–265.

Zhuo, Y., Zhou, T. G., Rao, H. Y., Wang, J. J., Meng, M., Chen, M., Zhou, C., & Chen, L. (2003). Contributions of the visual ventral pathway to long-range apparent motion. *Science, 299,* 417–420.